REPORT DOCUMENTATION PAGE

AD-A230 963

1. AGENCY USE ONLY (Leave blank)	2. REPORT DATE 23 January 1990	3. REPORT TYPE AND DATES COVERED Meeting Speech

4. TITLE AND SUBTITLE
Second-Generation System for Three-Dimensional
Imaging Using a Single Laser Pulse

5. FUNDING NUMBERS
C-F19628-90-C-0002
PE-63220C

6. AUTHOR(S)
F.J. Knight, D.I. Klick, M. Holz,
D.P. Ryan-Howard, and J.R. Theriault, Jr.

7. PERFORMING ORGANIZATION NAME(S) AND ADDRESS(ES)

Lincoln Laboratory, MIT
P.O. Box 73
Lexington, MA 02173-9108

8. PERFORMING ORGANIZATION REPORT NUMBER

MS-8522

9. SPONSORING/MONITORING AGENCY NAME(S) AND ADDRESS(ES)

Naval Sea Systems Command
High Energy Laser Project Office
Washington, DC 20362

10. SPONSORING/MONITORING AGENCY REPORT NUMBER

ESD-TR-90-162

12a. DISTRIBUTION/AVAILABILITY STATEMENT

Approved for public release: distribution is unlimited.

12b. DISTRIBUTION CODE

DTIC
ELECTE
JAN 15 1991
S D
B

13. ABSTRACT *(Maximum 200 words)*

This paper describes the design of a second-generation version of an optical detector capable of producing a 3-D image using a single laser pulse. The method consists of detecting reflected light from an object illuminated by a short laser pulse using a detector that provides high temporal resolution for each spatially-resolved pixel. The detector utilizes a fiber optic image converter to transform a square focal plane into a line array that projects onto a streak camera to obtain high time resolution in all the pixels. Both versions have a 16 × 16 angular field and a range resolution of 4 cm. The second-generation version incorporates a new fiber optic converter utilizing a binary optic input to improve focal plane coverage and smaller fiber cores to improve the angular resolution. This work builds upon our results reported in March 1989 at the Laser Radar IV SPIE conference.

14. SUBJECT TERMS

second-generation system   fiber optic converter
3-D image

15. NUMBER OF PAGES
13

16. PRICE CODE

17. SECURITY CLASSIFICATION OF REPORT	18 SECURITY CLASSIFICATION OF THIS PAGE	19. SECURITY CLASSIFICATION OF ABSTRACT	20 LIMITATION OF ABSTRACT
Unclassified	Unclassified	Unclassified	

ESD–TR–90 16 2

Paper presented at the SPIE/SPSE Symposium
Electronic Imaging
Conference 1260: Sensing and Reconstruction of 3D Objects and Scenes
Santa Clara, CA
11-16 February 1990

91 1 14 021

Second-generation system for
three-dimensional imaging using a single laser pulse

Frederick K. Knight, David I. Klick, Michael Holz,
Danette P. Ryan-Howard, and Joseph R. Theriault, Jr.
Massachusetts Institute of Technology, Lincoln Laboratory,
P. O. Box 73, Lexington, MA 02173

ABSTRACT

This paper describes the design of a second-generation version of an optical detector capable of producing a 3-D image using a single laser pulse. The method consists of detecting reflected light from an object illuminated by a short laser pulse using a detector that provides high temporal resolution for each spatially-resolved pixel. The detector utilizes a fiber optic image converter to transform a square focal plane into a line array that projects onto a streak camera to obtain high time resolution in all the pixels. Both versions have a 16 × 16 angular field and a range resolution of 4 cm. The second-generation version incorporates a new fiber optic converter utilizing a binary optic input to improve focal plane coverage and smaller fiber cores to improve the angular resolution. This work builds upon our results reported in March 1989 at the Laser Radar IV SPIE conference.

1. INTRODUCTION

This paper describes improvements to a detector[1] that uses a light pulse reflected off an object to image it in three dimensions: two in angle and one in range. The light pulse must be short enough to resolve the object in range, e.g., a 1 ns pulse yields 15 cm resolution. The detector then images the returned light *as it arrives from different parts of the object.* Figure 1 shows this procedure schematically using a cone as the target. Currently the detector has 4 cm range resolution and an angular field composed of 16 × 16 elements. The output of the detector is the intensity value of each pixel in the image for each range bin, that is, for each 4-cm slice on the object perpendicular to the laser illumination direction. Taken together these intensity values can be used to reconstruct the 3-D outline of the object. All of the necessary information is recorded during the time that the reflected light reaches the detector, that is, twice the time it took for the light pulse to pass the object. A streak camera provides the required time resolution. This paper reviews the detector performance as reported previously[2] and describes improvements being implemented.

The concept of 3-D image formation based on angle-angle-range data was originated by Courtney-Pratt[3] in 1982. He considered capturing successive frames from a camera with up to 1 ns time resolution but did not suggest the use of a fiber optic image converter. Other researchers[4,5] have detected single inputs from optical remote sensing using streak cameras. The new aspect of the present work is the use of multiple input channels for the streak camera to provide angular resolution as well as time resolution for optical remote sensing. The earliest proposal to use fiber optic converters to provide multiple inputs to an electronic streak camera was by Kapany[6] published in 1967. As early as 1976, a 7 x 7 square-to-slit fiber optic image converter was used as the input to a streak camera for X-ray imaging in laser fusion diagnostics[7]. Lear[8] described a system with 125 independent channels at the streak camera input, which was capable of remote use for weapons testing. Reedy[9] published an extensive analysis of fiber optic converters. Wilke and King[10]
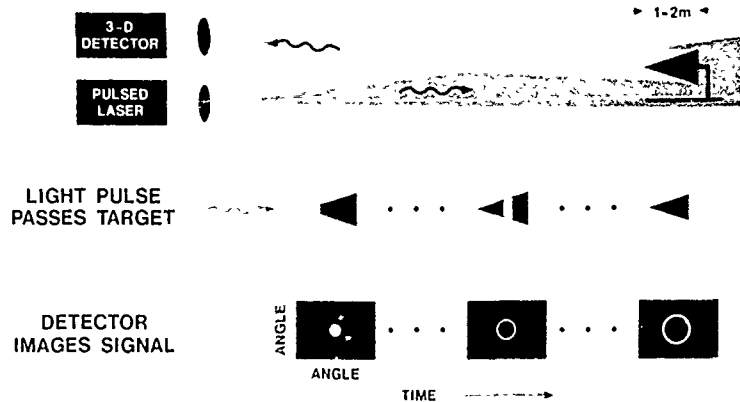
Figure 1: A laser pulse illuminates a cone viewed nose-on. The pulse's duration is less than the cone's depth. The reflected light can be detected (imaged in angle and resolved in time) to reveal the cone's characteristics.

reviewed tomographic uses of streak cameras in nuclear diagnostics, which include transforming 3-D data to 1-D using fiber optic converters. To our knowledge, our work is the first application of a streak camera with a fiber optic converter to the acquisition of 3-D data from optical remote sensing.

2. FIRST-GENERATION SYSTEM

The first-generation system was designed to obtain the best possible range and angular resolution over the widest wavelength range in the visible and ultraviolet using current technology. Figure 2 shows a block diagram; Fig. 3 is a photograph. The configuration of the system is dictated by the desire to achieve the best possible range resolution. Mode-locked lasers are available that provide very short (tens of ps or less) illumination pulses. The fastest available detector is a streak camera, which works by rapidly sweeping the photoelectrons generated at the input photocathode across an output phosphor. If the photocathode input consists of a time-varying light signal confined to a point, the streak camera output is a streak of light with distance along the streak corresponding to time and intensity along the streak corresponding to the input intensity at each moment in time. Streak cameras are generally able to sweep a number of such input points of light entering along a line coincident with an input slit or along a wire grid, generating a 2-D field at the output phosphor.[11] A fiber optic array converts the 2-D focal plane into a 1-D line array, which is then imaged onto the slit at the photocathode of the streak camera using relay optics. We stress the state of the art by having 273 (16 × 16 + 17 for calibration) input elements. Each of these elements produces a light streak at the camera output. An intensified TV camera reads the resulting 2-D field of data into a computer, which processes the 2-D field to reconstruct a 3-D image of the object. We call the reconstruction an angle-angle-range (AAR) image of the object.

The raw data read from the SIT tube and stored in the computer are a 2-D array of pixels as shown in Fig. 4. The abscissa is time over the fraction (f = 80%) of the streak camera sweep, t_{sweep}, imaged through the image intensifier, or a range extent equal to

$$R = c \times t_{sweep} \times f/2 \qquad (1)$$

where c = 30 cm/ns is the speed of light in air. For t_{sweep} = 25 ns and f = .8, R is 3 m, a convenient range extent for imaging meter-size targets in our laboratory. This time is sampled with about 5 pixels per resolution element (FWHM), which is currently 250 ps or about 4 cm. Thus, over the 20 ns of imaged
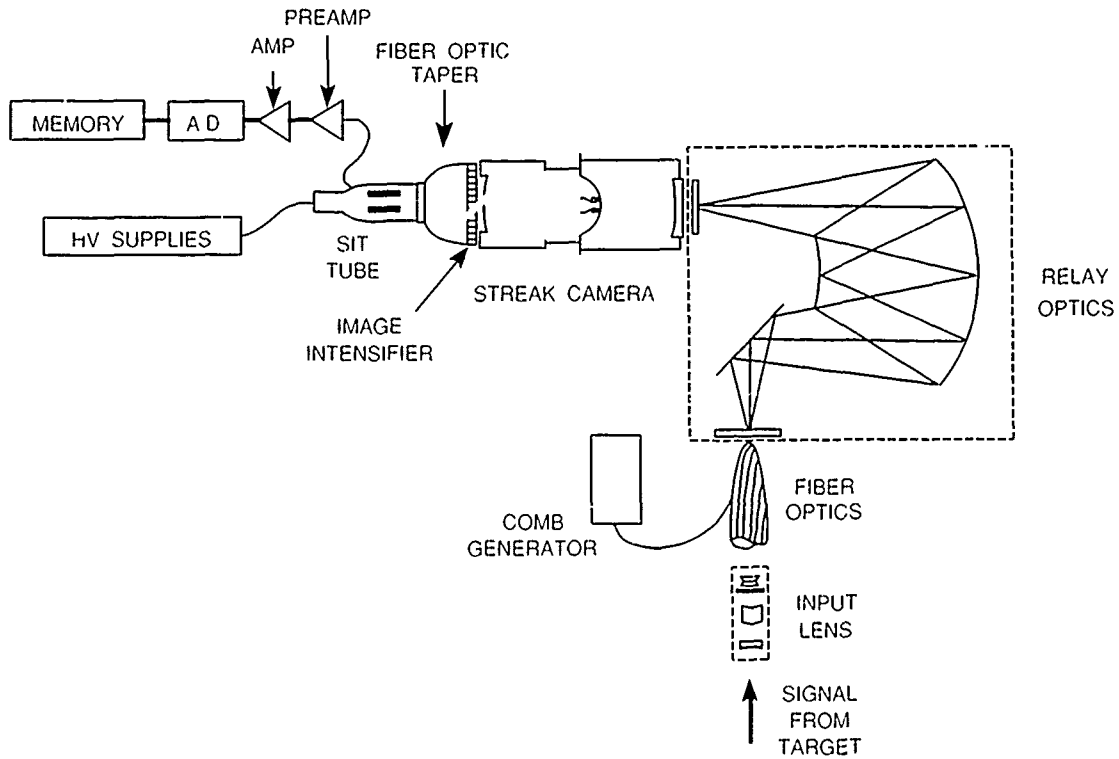
Figure 2: Block diagram of first-generation system. The signal is the light from a pulsed laser reflected off the target and is focussed on a focal plane dissected by a fiber optic array. The array is converted into a line, which is relayed to the streak camera photocathode. The streak camera resolves the light from all fibers in time and stores the information on a phosphor screen where it is read out to a memory.
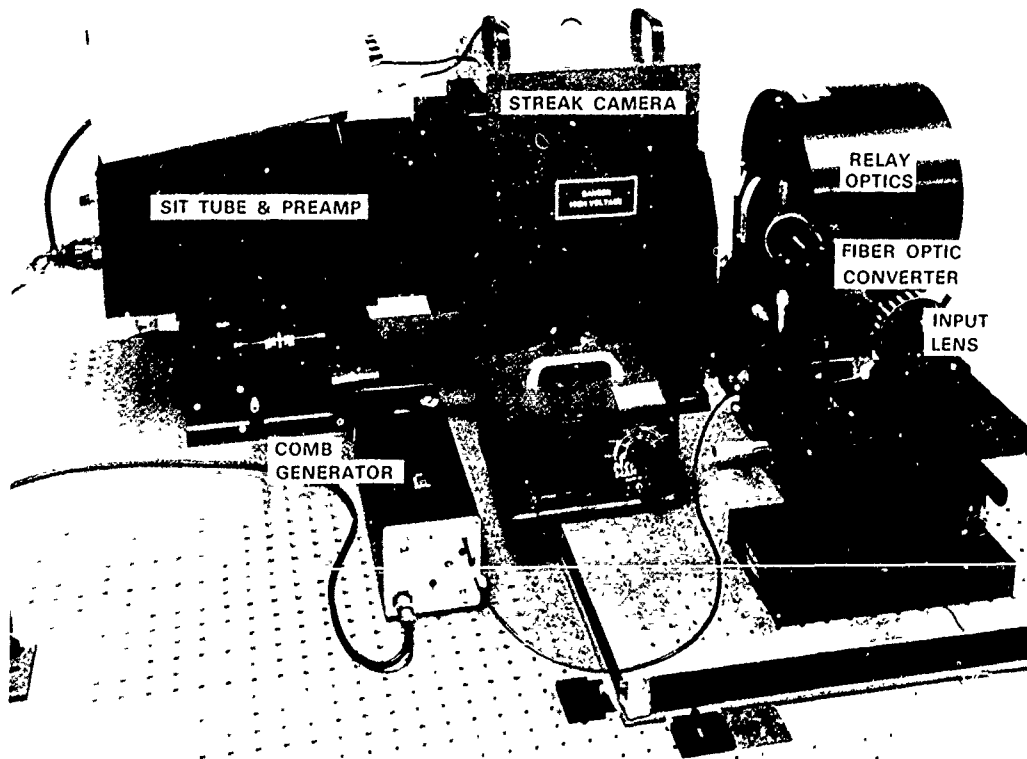

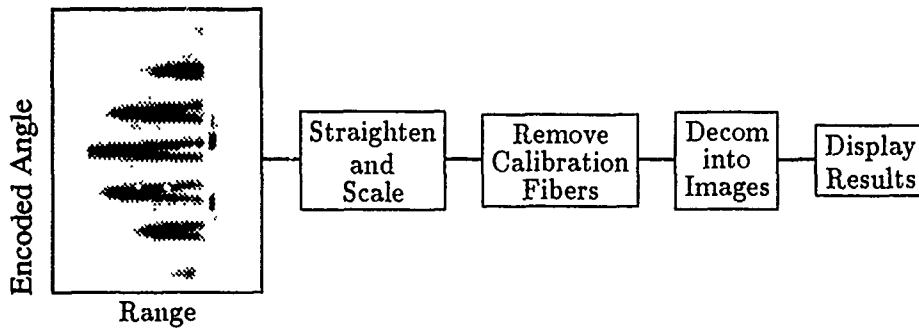Figure 3: Photograph of first-generation system

Figure 4: Data processing block diagram for 3-D imaging.

sweep, there are about 400 pixels of 50 ps duration for an image depth of 3 m. The ordinate is the output from the fiber optic converter or encoded angular information from the focal plane of the input lens. The encoding is a vertical weave starting in the upper left corner of the focal plane and looping back and forth to the upper right, so that in the raw data the leftmost column is at the top and rightmost is at the bottom. Interspersed between the columns are single calibration fibers. Thus the output column consists of a sequence of one calibration fiber, 16 fibers starting from the top of the leftmost column of the focal plane, one calibration fiber, 16 fibers starting from the bottom of the next column of the focal plane, one calibration fiber, *etc.*—a total of 273 fibers. Seven and four of the calibration fibers are ganged together in two bundles, each of which can be connected to a periodic laser diode (a comb generator). The other six are dark fibers. Since the image intensifier images about 80% of the fibers, the edges of the focal plane are lost. The imaged fibers are sampled at $\approx$ 2 pixels/fiber on the SIT tube. In summary, the raw data consist of a series of short time slices of the focal plane encoded to vertical columns.

The raw data can be processed to varying degrees depending on what information is needed. Complete processing requires three major steps, as Fig. 4 shows. The first removes the distortions introduced by the streak camera and the SIT tube and reduces the raw data to 1 pixel per fiber along the ordinate and 1 pixel per time FWHM along the abscissa. The second removes the calibration fibers. If the comb output is present, residual light remains in neighboring pixels due to the finite resolution of the system. The third reconstructs the focal plane for each range bin (each column) in the data.

Figure 5 shows the processed data for a flame-sprayed aluminum cone (175 cm long $\times$ 50 cm in diameter) viewed nose-on. The data are displayed using slices along the three dimensions: range, vertical angle, and horizontal angle. Along range, the slices are annuli indicating the diameter of the cone along its axis. The images are smeared over multiple pixels due to the system angular resolution, and the intensity varies around each annulus due to incomplete focal plane coverage by the fiber cores. The slices in angle indicate the cone's outline. There are about 50 range bins along the cone, yielding fine rendition in range. The cone's base spans seven angular pixels, yielding cruder angular resolution. In spite of the rather crude angular resolution and the intensity variation, the images in the slices are well-defined, and one can see the 3-D nature of the cone. This simple target demonstrates the ability of the AAR detector to image in three dimensions *using a single laser pulse*.

3. PROBLEMS AND REMEDIES

Several problems with the first-generation system were noticed when data were collected. The design of the second generation system (described in the next section) remedies some of these problems. The data in Fig. 5 demonstrate two of the problems addressed: poor angular resolution and loss of signal.

While an angular coverage of 16 $\times$ 16 pixels approaches the limits of streak camera spatial resolution, Fig. 5 shows that full separation of pixels is not attained even at this achievable angular resolution. The horizontal resolution is better than the vertical resolution because fibers carrying signal from neighboring vertical pixels are adjacent at the line end of the image converter. Fibers carrying signal from neighboring
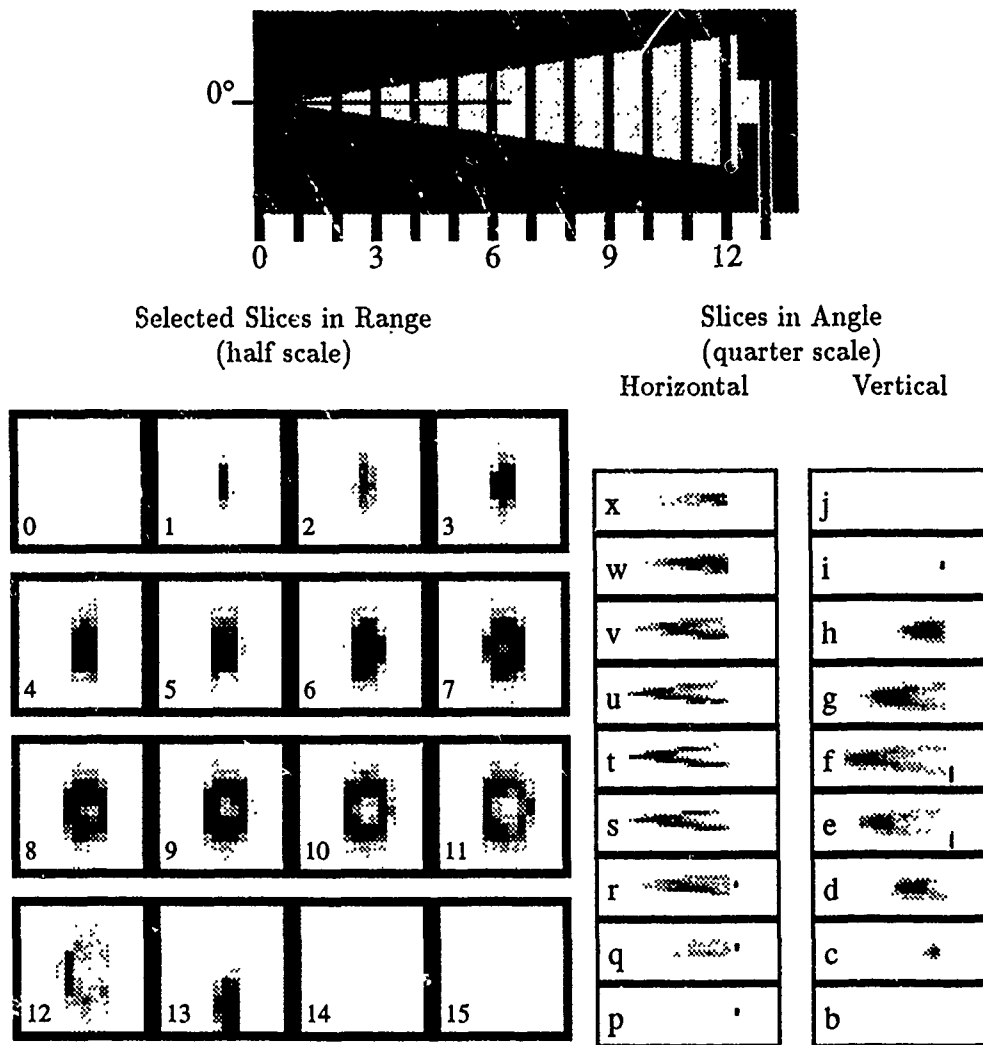
Figure 5: AAR data for a flame-sprayed aluminum cone illuminated nose-on (0°). The cone is shown from the side (left top) and from the rear (right top). The range slices (left bottom, 0-15) are selected as shown on the top and correspond to every fourth FWHM-range-bin. The slices along horizontal angle (n dle bottom, p-x) are slightly narrower than the slices along vertical angle (right bottom, b-j) due to the finite system resolution. The target holder is behind the base.

horizontal pixels are separated by 16 other fibers. Figure 6 illustrates part of the line (output) end of the image converter. In the first-generation system (Fig. 6a), large-core thinly-clad fibers were used, and as a result, the cores are not well separated. The line end is imaged (by the relay optics and the streak camera electron optics) without magnification to the streak camera output phosphor, where blurring of the light from closely-spaced cores can occur.

To remedy the problem of blurring of light from adjacent fibers, leading to poor vertical resolution, two alternate designs were advanced for the image converter line end. Figure 6b shows the use of smaller fibers (4 times smaller outer diameter), with each fiber that carries signal separated by three dead fibers. This confines the signal to small areas on the streak camera phosphor, which reduces blurring. Unfortunately, working with small diameter fibers is more difficult, and they break easily. Consequently, the design of Fig. 6c was chosen for the line end of the second-generation image converter. Here, the outer diameter is the same as in the first-generation system, but the core diameter is smaller. Standard cladding-to-core diameter ratios were used for both systems: 1.2 for the first generation and 2.5 for the second generation. Now, areas of the streak camera phosphor containing signal will be well separated, reducing blurring. Use
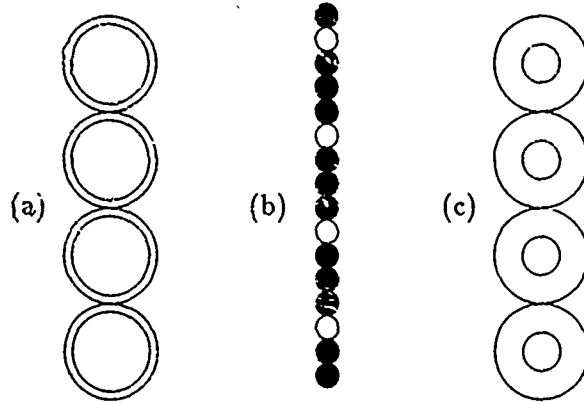
Figure 6: *Possible configurations of the fiber optic converter at the line (output) end. First-generation arrangement (a) has large cores and thin cladding. Possible improvements employ small fibers separated by dead fibers (b) or thickly-clad, small-core fibers (c), as used in the second-generation system.*
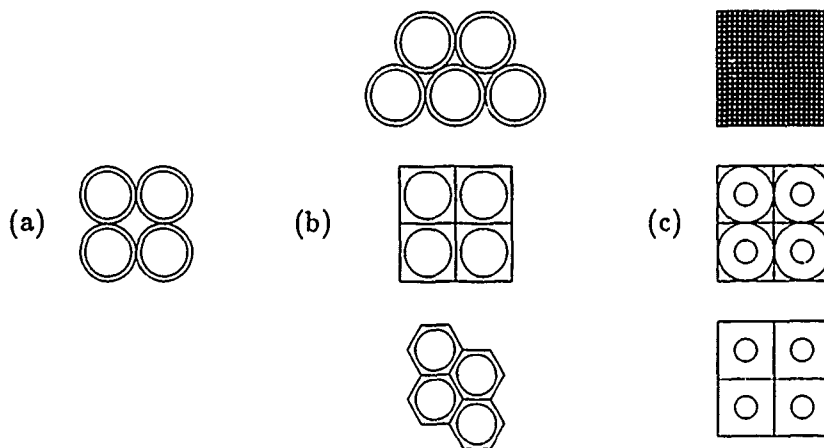

Figure 7: *Possible configurations of the fiber optic converter at the array (input) end. First-generation arrangement (a) has large-core fibers packed in a square array. Closer packing arrangements (b) are possible to reduce light loss. Large dead spaces can be avoided by using fiber bundles (c, top) or, as in the second-generation system, with binary optics (c, middle and bottom).*

of small-core fibers will also reduce blurring in the sweep direction, improving time (range) resolution.

The problem of loss of signal is evident in the data of Fig. 5, for example, images 9-12. The signal for one FWHM range bin forms a thin annulus, but when viewed through the first-generation system, the image is not azimuthally symmetric. Artifacts appear, either bright patches or holes in what should be a continuous ring. One reason for the occurrence of these artifacts can be seen in Fig. 7a, which represents a segment of the square fiber array at the first-generation image converter input. Due to both the cladding and the gaps between fibers, 45% of the input signal is lost. If the annular signal passes over a fiber core, a bright patch will appear in the image, but if it passes over a gap between fibers, no signal will be recorded at that spot in the image. Some of this signal could be recovered by the schemes of Fig. 7b, where fibers are packed more closely. However, dead spaces remain, still leading to artifacts.

In the schemes of Fig. 7c, there are no large gaps. The arrangement at the top uses fiber bundles. A large fraction of the signal is still lost here, but all the gaps are miniature, and each pixel is evenly sampled. The middle and bottom arrangements of Fig. 7c employ binary optics.[12] Here each pixel is spanned by a square lenslet that collects light input from the entire pixel area and focusses it to the center of the square. At the center is a small fiber core, as is optimal at the line end. In one case (middle), fibers with large
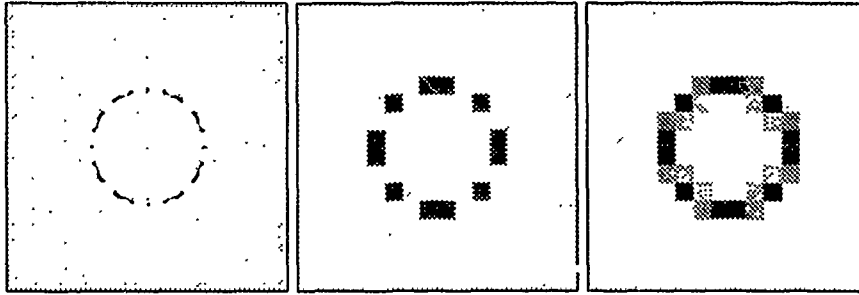
Figure 8: First-generation system performance and expected improvement in the second-generation system. The incomplete coverage of the focal plane (left) in the first-generation system produces azimuthal variation in intensity for the azimuthally-symmetric cone viewed as in Fig. 5 (middle). The binary optic of the second-generation system channels light from the entire focal plane into the fiber cores (right).

outer diameters abut as in the first-generation system. In the other case (bottom), small-diameter fibers are held in place in holes in a metal block. Due to the difficulty of working with small-diameter fibers, the middle scheme of Fig. 6c was chosen for the second-generation system. Using binary optics produces a uniform spatial sampling of the signal entering each pixel.

The difference in image quality expected from this improvement is shown in Fig. 8. At the left is the annular signal from the base of the cone of Fig. 5 superimposed on the first-generation image converter input array. At the center is the calculated image, assuming 100% spatial sampling over the active areas: the circular fiber cores. At the right is the corresponding image for a second-generation system employing binary-optic lenslets. Artifacts are reduced in the second-generation system. However, even with no loss of signal, pixels are not evenly illuminated due to the changing fraction of the annulus present in each pixel The registration of the annulus to the square grid still affects the image obtained. Nonetheless, since all the signal is detected, smoothing can be performed, assuming continuity in the target surface. These considerations of the fidelity with which the image is preserved become more important when one attempts to reconstruct objects more complex than a Lambertian cone.

4.   SECOND-GENERATION SYSTEM

Figure 9 provides a side view of the optics of the second-generation system. As with the first-generation system, 2 m scale targets will be imaged at a distance of 10 m with a lens of focal length 2.54 cm. However, instead of a fiber array at the image plane, a binary optic lenslet array will dissect the image. This improves the system by producing a uniform spatial sampling on the focal plane, but, as we see below, reduces the system speed to $\mathcal{F}/10$. Each lenslet will focus light from its portion of the image onto the core of its corresponding fiber. Figure 10 shows the second-generation fiber array and binary optics in more detail. Fig. 10a is a front view of the array, which will be constructed from 16-fiber-wide ribbons interleaved with shims. The shims provide ease of manufacturing and more precise alignment of the fiber ribbons. Use of the shims is made possible in the second-generation array by the ability of the binary optic lenslet array to conform to any desired shape, in this case, a rectangle.

4.1.   Design considerations for second-generation optics

Placing a matched array of lenses in front of the fiber-optic converter—one lenslet centered on each fiber—produces a number of practical benefits, all derived from the principal advantage of having light gathered over the entire aperture of the lenslet and thereby achieving uniform spatial sampling. As shown in Fig. 9b, each lenslet serves as a field lens, relaying light falling within the acceptance cone of the entrance aperture into a *smaller* exit aperture matched, ideally, to the core area and acceptance cone of the fiber. The fiber entrance face is placed one lenslet focal length behind the array, which in turn is located at the focal plane of the input lens.
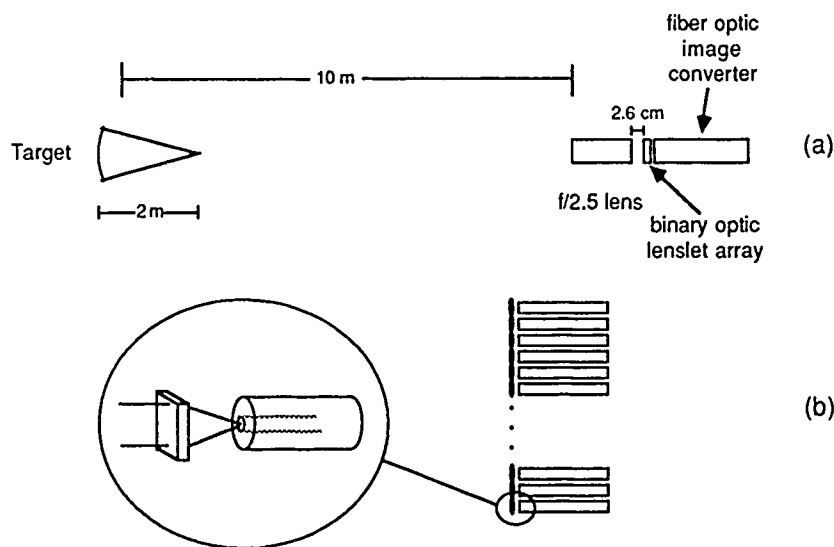
Figure 9: *Layout of the second-generation input optics. (a) The target is imaged onto a binary-optics lenslet array with a lens. (b) Each lenslet focusses light from a rectangular portion (pixel) of the image onto the fiber core.*

By inserting such an optical concentrator, we can use a practical⁻ ᵒber layout for the converter with moderate ratio of fiber core to unit cell area and still avoid samμ ᵍ artifacts, reduce crosstalk, and maintain a reasonable overall light collection efficiency of the detection system. We characterize the spatial sampling by the term "fill factor," given as the ratio of the sampled area to total unit cell area; for the design illustrated in Fig. 10 the fill factor is 6.8%.

In the art c˙ light concentrator design, the brightness theorem is a fundamental principle: light flux, *i.e.*, the intensiιy̆ per unit solid angle, is conserved in any passive optical system.[13] As we compress the light to a smaller area, its divergence increases. Thus, the specification of the concentrator requires two steps: 1) matching in angle and 2) matching in area.

Let us first "match in angle." The numerical aperture of the fiber corresponds to $\mathcal{F}/2$. From this follows the focal length of the relay lenslet as 585 μm by requiring that the field of view of the fiber match the diagonal of the rectangular unit cell with 180 × 230.8-μm sides. Given the focal length of the field lens, the 60-μm diameter of the fiber, and assuming perfect placement of each fiber, we can satisfy the "match in area" by setting the $\mathcal{F}$-number of the input lens to $\mathcal{F}/9.8$ (= 585 μm/60 μm). If the fibers are spaced with a small error ϵ, the effective diameter of the fiber would be reduced to 60 − 2ϵ μm and the speed reduced by a factor $\left(1 - \frac{\epsilon}{30 \, \mu m}\right)^{-1}$.

What techniques are available to fabricate a microlens array, 16×16 elements in a rectangular 180×230.8-μm format with 100% fill factor and $\mathcal{F}/2$ speed? Highly regular *refractive* microlens arrays with $\mathcal{F} < 6$ have been demonstrated, for example, by exploiting conformational changes in a specific class substrate[14] or by melting photolithographically-defined posts of photoresist.[15] In our application these approaches suffer the drawback that the lenslet aperture would be restricted to spherical shape, giving a fill factor of only about 60%. A photolithographical mass transport process might circumvent this restriction, while retaining refractive lenslets, but only in a specific substrate material.[16] Alternatively, we could use a *diffractive* lenslet technology—binary optics—that has proven its value in microlens applications, such as diode laser array collimation[17] or beam steering[18] and can, in particular, satisfy the 100% fill factor requirement easily. We have developed binary optics in-house, and, therefore, it is our fabrication method of choice.
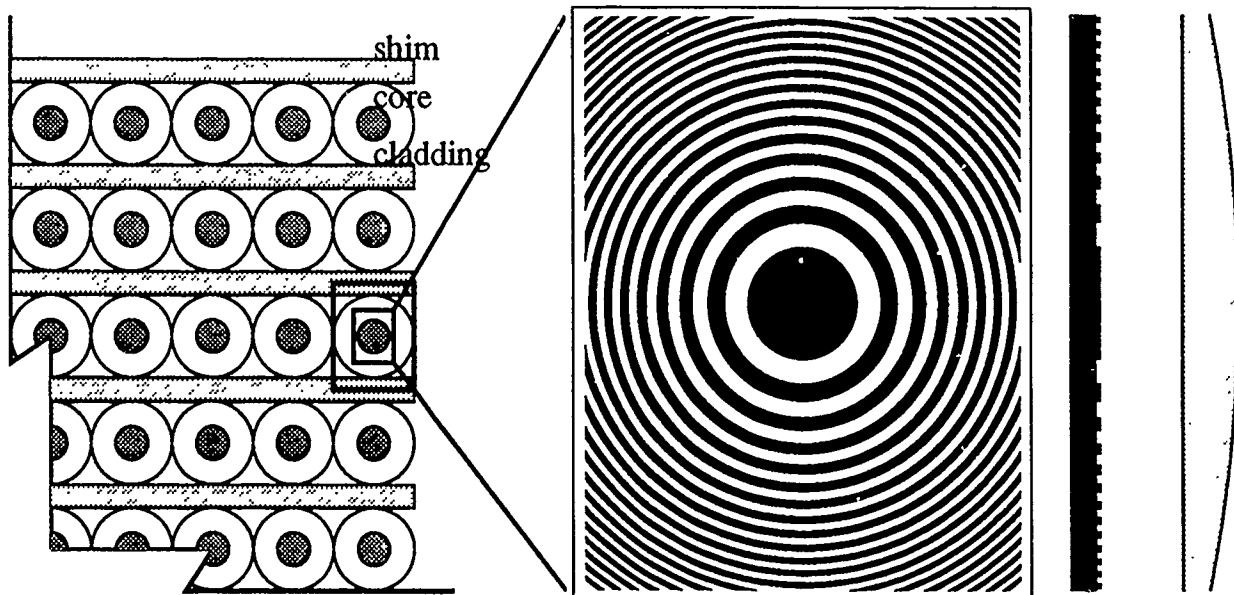
Figure 10: Second-generation fiber optic converter and binary optics. The input end of the fiber optic array is covered with binary optic lenslets (left). One lenslet's boundary is shown (outer rectangle) and a portion (inner rectangle) is enlarged to show the binary mask contours from the front (left center) and side (right center). For the $\mathcal{F}/2$ lens at $\lambda = 0.532$ μm, the central zone has a diameter of 35.2 μm. The binary optic is fabricated by etching the marked pattern as a plane profile into the substrate and performs the function of the glass lens shown at the far right.

4.2. Binary optic lenslet array

Binary optics is an effective approach for microlens array implementation. It is a diffractive optics technology that utilizes specific surface-relief structures, high-resolution lithography, and reactive ion-beam etching techniques to transfer the relief pattern into a dielectric substrate.[12] A single etching step produces a two-level—"binary"—surface. For on-axis lens-like applications, multi-level relief structures achieve high diffraction efficiency by approximating the desired continuous phase surface in a step-wise manner obtained from repeated application of the binary etching process at different depths and widths. Every etch doubles the number of phase levels, and a small number of etches can produce a highly efficient lenslet; for example, three etching steps result in an eight-level lens with a theoretical efficiency of 95%.[19]

The fabricational advantages of photolithographically defining diffractive microlens array structures have been appreciated for some time.[20] Multi-level, high-speed lenslets in the visible, however, require lithography with up to $\frac{1}{10}$-μm precision. We note that the smallest ring of a Fresnel lens is given by $2\lambda\mathcal{F}$-number. The lenslet shown in Fig. 10 has a speed of $\mathcal{F}/2$ in the diagonal, resulting in smallest features of about 1 μm size for a binary and 0.5 μm for a four-level implementation. Such lenslets would achieve a theoretical efficiency of 41% or 81%, respectively. We have not made a final decision on fabricating a two- or four-level array. In either case, however, we will retain the principal advantage of the microlens array: the sampling of the input light flux uniformly across the entire focal plane.

4.3. Image converter

The second-generation fiber optic image converter is similar to the first-generation one, except for the use of smaller-core fibers and shims. The fiber outer diameter remains 180 μm, so that the output line of 273 fibers is 50 mm long, the same as the slit at the streak camera photocathode. With a cladding-to-core ratio of 2.5, the core diameter is now 60 μm. At the input end, fibers are arranged in a rectangular array and separated in the horizontal dimension by shims of 50.8 μm thickness. The overall array dimensions

are 3.69 mm (horizontal) × 2.88 mm (vertical). UV-transmitting fibers with numerical aperture of 0.25 are used. Fiber lengths are identical so as not to introduce timing errors. Lengths are kept short (about 0.3 m) to minimize spatial mode dispersion. The 17 calibration fibers are ganged into a bundle 900 μm across. Pulses from the laser diode in the comb generator are routed to the calibration bundle via a 1 mm core cable. The cable is subjected to bends that promote excitation of all spatial modes, spreading the light to all the calibration fibers in the bundle.

The image converter output line of fibers is imaged with unity magnification onto the curved photocathode by means of an Offner relay. Reflective elements are employed to allow operation throughout the UV-visible spectrum (250 - 850 nm). If UV operation were not required, several simplifications could be implemented. The streak camera quartz faceplate could be replaced with a fiber optic faceplate. The Offner relay would then be unnecessary, as the fiber optic image converter could be butt-coupled to the fiber optic faceplate. UV transmission would not be required of the input lens, the binary optics, nor the fiber optics.

4.4. Expected performance

To quantify the improved resolution expected with the second-generation system, we recalculated a model tested successfully[2] for the first-generation system. The model combines the modulation transfer functions (MTF's) of the components to predict the system response. The model for the first-generation system predicted slightly better response than observed using calibration data.[2] Expressed in terms of the spatial frequency ν at the focal plane of the input lens, the MTF of the first-generation system begins to decrease from unity at 1 lp/mm, has a range of values from $1 \leq \nu(\text{lp/mm}) < 5.56$, and is always zero for $\nu \geq 5.56$ lp/mm. Here we define 1 lp/mm as a line pair consisting of 0.5 mm black bar followed by a 0.5 mm white bar. The limiting element is the fiber optic converter. We expect that the second-generation system will improve the system MTF, as well as collect significantly more of the light falling on the focal plane. With the introduction of the binary optic, the fiber optic converter has a square-well response, so its MTF is $\sin(\pi z)/(\pi z)$ where $z = \nu/\nu_{0x,y}$ and $\nu_{0x} = (180\mu\text{m})^{-1} = 5.56$ lp/mm along the fiber ribbons and $\nu_{0y} = (230.8\mu\text{m})^{-1} = 4.34$ lp/mm perpendicular to the ribbons. Figure 11 shows the MTF's of all the components of the second-generation system. The fiber optic converter is still the resolution-limiting element. This is an improvement—the best that can be done with a 16 × 16 fiber array (using 180 μm diameter fibers), which contains about the largest number of fibers that can be resolved by one streak camera.

5. SYSTEM CAPABILITIES FOR 3-D IMAGING

The first-generation angle-angle-range system demonstrated the feasibility of recording 3-D images using a single laser pulse to illuminate the target. The second-generation system will improve the angular resolution and the light-collecting efficiency. In this section, we discuss other improvements that are possible and their importance in using the system.

Our original motivation for this system was to use it as a receiver for active, optical remote sensing. laser radar utilizing a short-pulse laser to illuminate a distant target. Other possible applications are robotics where an instantaneous 3-D image is helpful, laser diagnostics where time-resolved images could indicate the history of mode development (at a fixed plane) or transient behavior, and real-time imaging of surface features where images could be used to monitor some time-dependent process that produces variation in reflectivity. The latter two treat the "range" dimension as time. The AAR system is suited for these because it has the ability to acquire images in rapid succession and store them for analysis. For all of these applications high temporal resolution along with imaging is required, but the imaging capability is limited by the number of inputs to the streak camera (or, equivalently, the number of fibers or parallel channels). Here we discuss ways to better utilize the temporal and imaging capabilities of the system. We suggest improvements in the system and alternative approaches that could make the system more suited for a particular application.
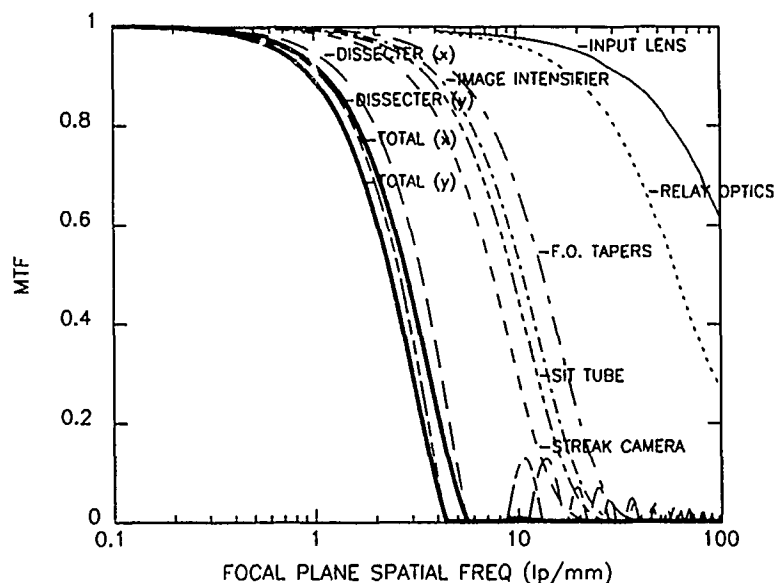
Figure 11: Modulation transfer function of the second-generation 3-D imaging system. The "TOTAL (x)" refers to the total MTF along the fiber ribbons; the "TOTAL (y)" perpendicular to the fiber ribbons.

There are ways to improve the range resolution from its current value of 4 cm FWHM. This is equivalent to increasing the time resolution of the system, which is important for resolving finer features in time or in range. The streak camera sweep time could be decreased to ≈ 1 ns, yielding 10 ps resolution. Use of such a sweep time would mean the system time resolution would be limited by the laser pulse width, which could be reduced from 100 ps to 10 ps by changing the intracavity etalon and the passive dye used for mode-locking. The result would be a 25× improvement in range resolution, from 4 cm to 1.6 mm. Thus, objects of 25× smaller scale could be resolved in the range dimension. Since the resolution is independent of distance to the target, the maximum distance would be limited by the achievable signal-to-noise.

The angular resolution on the target is limited to about 16 pixels across the field of view, but there are ways to improve resolution on the target within this constraint. First, the input lens controls the field of view, so using several lenses having different focal lengths or a zoom lens would allow varying the field of view to accommodate targets of various angular extents. In particular, one could "zoom in" on portions of a target, after imaging the full target, to study small-scale features. Simultaneous imaging using a high-angular-resolution, angle-angle camera could accomplish the same thing, at the expense of giving up range resolution. Second, two or more streak cameras, suitably synchronized, could share the recording of a field of view with a larger number of pixels. Third, views from different directions, either taken simultaneously with multiple AAR systems or taken consecutively while waiting for the target to present other views to a single system, could resolve more parts of the target and overcome shadowing. If the target is cooperative and close, taking many views would provide AAR data to use as input to tomography,[21] which could confirm the existence of surface features not clearly resolved in a single AAR view. A higher repetition rate could aid this process. Currently the data acquisition rate is limited by the laser pulse repetition frequency (20 Hz) and the data transfer rate to the computer (750 kHz or 12 frames/s). Both of these could be increased significantly. A higher transfer rate would also allow a significant improvement in the resolution of the readout system, e.g., to sample each FWHM pixel above Nyquist rate and allow centroiding. All of these improvements are possible with existing technology.

Further image processing, beyond that necessary to process the raw data as shown in Fig. 4, could enhance the results. Using assumptions about the target structure, e.g., continuity across its surface or convexity, the application of smoothing or sharpening of the images could indicate more about the 3-D nature of the target. The set of data from a single laser pulse could be used as input to an object-recognition program to compare the target with 3-D shapes. Comparison of angle-angle images, having high angular resolution, with AAR data, having high range resolution, could refine estimates of target shape, e.g., to

calculate low-order moments of the AAR data. Image processing could be implemented in hardware to reduce the data transfer rates and data storage requirements.

6. SUMMARY

This paper reviews the performance of a 3-D imaging system and describes modifications being implemented to improve the performance. The system images the light reflected off a macroscopic target and resolves it in time, as the reflected light arrives from the target. The illumination must come from a pulsed source, whose pulse length is shorter than the depth of the target along the line of sight. The output is intrinsically three dimensional (in angle and range) and, thus, can be used to infer 3-D shape. The angular field has 16×16 elements, and the resolution in the range dimension is 4 cm. Current modifications are 1) addition of binary optics to collect all the signal at the focal plane and 2) reduction in the core diameter of the fiber optics to improve angular and range resolution. Applications include active remote sensing, robotics, and laser diagnostics.

7. ACKNOWLEDGEMENTS

8. REFERENCES

1. Fred Knight and Ken Kalata, United States Patent Number 4,791,490.

2. F. K. Knight, D. I. Klick, D. P. Ryan-Howard, J. R. Theriault, Jr., B. K. Tussey, A. M. Beckman, "Three-dimensional Imaging Using a Single Laser Pulse," *SPIE*, **1103**, 174-189 (1989).

3. J. S. Courtney-Pratt, "High speed photography to provide a three dimensional view," *SPIE*, **348**, 254-259 (1982).

4. J. B. Abshire and J. E. Kalshoven, Jr., "Multicolor Laser Altimeter Barometric Measurements over the Ocean: Experimental," *Applied Optics*, **22**, 2578-2585 (1983).

5. A. Ferrario, P. L. Pizzolati, and E. Zanzottera, "Time resolved LIDAR fluorosensor for oil detection," *SPIE*, **701**, 234-235 (1986).

6. N. S. Kapany, *Fiber Optics Principles and Applications*, Academic Press, New York, 268 (1967).

7. J. C. Cheng, L. G. Multhauf, and G. R. Tripp, "Fiber Array Technique for Subnanosecond X-ray Framing Camera," *SPIE*, **97**, 218-222 (1976).

8. R. Lear, "Fast Imaging Applications in the Nuclear Test Program," *IEEE Trans. Nuc. Sci.*, **NS-31**, 495-503 (1984).

9. R. P. Reedy, "Unique Components for Photonics Diagnostic Systems using Fiber Optics," *SPIE*, **648**, 99-126 (1986).

10. M. Wilke and N. S. P. King, "Two-dimensional Time-dependent Imaging Utilizing Tomographic Concepts," *SPIE*, **648**, 24-43 (1986).

11. James Chang, William F. Filter, Grant J. Lockwood, and Barry T. Neyer, "Photonic methods of high-speed analog data recording," *Rev. Sci. Instrum.*, **56**, 1861 (1985).

12. J. R. Leger, M. Holz, G. J. Swanson, and W. B. Veldkamp, "Coherent Laser Beam Addition: An Application of Binary-Optics Technology," *Lincoln Laboratory Journal*, 1, 2 (1988).

13. W. T. Welford and R. Winston, *The Optics of Nonimaging Concentrators*, Academic Press, New York, 1978.

14. N. F. Borelli, D. L. Morse, R. H. Bellman, and W. L. Morgan, "Photolytic technique for producing microlenses in photosensitive glass," *Appl. Opt.* **24**, 2520–2525 (1985).

15. Z. D. Popovic, R. A. Sprague, and G. A. N. Connell, "Technique for monolithic fabrication of microlens arrays," *Appl. Opt.* **27**, 1281–1284 (1988).

16. Z. L. Liau, V. Diaduk, J. N. Walpole, and D. E. Hull, "Large-numerical aperture InP lenslets by mass transport," *Appl. Phys. Lett.* **52**, 1859–1861 (1988).

17. J. R. Leger, M. L. Scott, P. Bundman, and M. P. Griswold, "Astigmatic wavefront correction of a gain-guided laser diode array using anamorphic diffractive microlenses," *SPIE* **884**, 82–89 (1988).

18. W. Goltsos and M. Holz, "Binary micro optics: an application to beam steering," *SPIE* **1052**, 131–141 (1989).

19. G. J. Swanson, "Binary optics technology: the theory and design of multi-level diffractive optical elements," *Lincoln Lab. Tech. Rep.* **854** (1989).

20. L. d'Auria, J. P. Huignard, A. M. Roy, and E. Spitz, "Photolithographic fabrication of thin film lenses," *Opt. Comm.* **5**, 232–235 (1972).

21. F. K. Knight, A. M. Beckman, D. I. Klick, D. P. Ryan-Howard, K. I. Schultz, J. R. Theriault, Jr., B. K. Tussey, "Two-dimensional tomographs using range measurements," *SPIE*, **999**, 269-280 (1988).